Korean J. Chem. Eng., **28**(8), 1651-1657 (2011)
DOI: 10.1007/s11814-011-0046-0

Dynamic modeling of paper drying processes

Chang Hoe Heo, Hyunjun Cho, and Yeong-Koo Yeo†

Department of Chemical Engineering, Hanyang University, Seoul 133-791, Korea
(*Received 13 September 2010 • accepted 21 February 2011*)

Abstract−A dynamic model describing the behavior of a multi-cylinder drying section in paper production plants was developed based on the mass and heat balances around drying cylinders. The balance equations consist of sets of differential equations describing heat and mass transfer around the canvas, the web and the drying cylinders. Values of cylinder temperatures and moisture contents were estimated and compared with operation data. To obtain further information for energy consumption, the generation of entropy at each drying cylinder was investigated based on the model developed.

Key words: Drying Section, Modeling, Simulation, Entropy Production

INTRODUCTION

A modern paper machine can be considered as a production line consisting of a stock preparation system, wire section, wet pressing, drying and coating units as shown in Fig. 1. In stock preparation, different raw materials such as chemical pulp from pulp mills, mechanical pulp from chip refiners, chemicals and additives are mixed together. Pulps are usually refined in order to achieve the required product quality. After it is cleaned and diluted, pulp stock is fed into the white-water system in the wire section of the paper machine.

The white-water system consists of the headbox, wire and the circulated white-water that is a filtrate from the wire. White-water is used to dilute the stock to the desired consistency (0.3-1%) for the paper web forming process. The headbox spreads the stock flow on the wire across the width of the machine and the paper web is formed. After that, water is removed first by wet pressing and then contact drying on steam-heated cylinders. Often, modern paper machines have on-machine coaters that apply pigment-coating color on the paper. Coating may be on both sides and even double or triple layered. In addition to these principal systems, there are several support systems such as for broke handling, chemical preparation and so on.

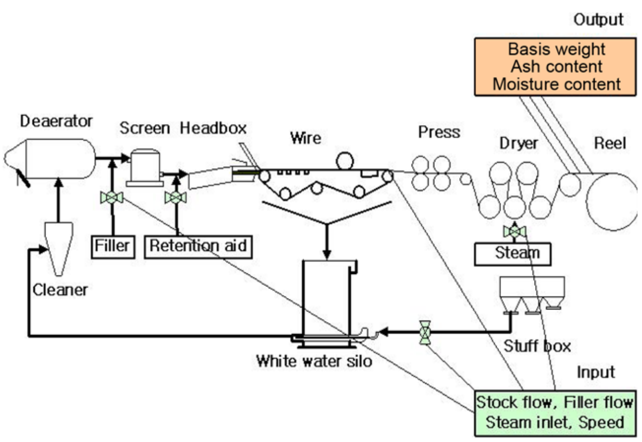

Fig. 1. Schematics of a paper machine.

A grade change is a product quality change on a paper machine. In a big grade change, several inputs to the paper machine are changed, for example, proportioning of raw materials, refiner loads, stock flows, headbox settings, machine speed, lineal pressures in wet pressing, steam pressures and coating settings. So far, the most common way to execute a grade change is by ramping. An open-loop method such as ramping suits grade change well because there are no exact target values for the basis weight and moisture. It is satisfactory if the target values hit inside an acceptance range after the grade change. Most grade changes are basis weight transitions. The basis weights in a production schedule are run in a cycle that is optimized so that the basis weight changes are as small as possible. The ideal condition is that the allowed ranges of sequential grades overlap. A typical grade change consists of a calculation of target values and a dynamic co-ordination of paper machine speed, pulp stock flow and steam. It is crucial to a successful grade change that the new target values are accurately known. Stock flow and machine speed together control both the production rate and basis weight.

The paper web moving out from the pressing part of the wet section contains fibers and solids (40-45%) and remaining water (55-60%). The remaining water is removed by heat supplied from drying cylinders in the drying section. Drying is controlled by steam pressure, but often only the last steam groups are used for control purpose. Because of long time constants and dead times in the drying process, the target values for steam pressures are the most important. Also, raw material properties, the condition of the paper machine, basis weight, moisture and speed, all affect the drying rate. The machine tender usually gets the initial target values from the records of the previous runs. The increasing interest in dynamics of the paper drying process has heightened the need for more detailed descriptions on the behavior of paper drying processes. The paper drying section consists of 30-70 drying cylinders and consumes a large amount of process steam. The primary reason for the interest

†To whom correspondence should be addressed.
E-mail: ykyeo@hanyang.ac.kr

in the drying dynamics is the enhancement of operation economics by the reduction of energy consumption. It can be achieved by the increase of evaporation efficiency followed by the reduction of the number of drying cylinders.

Utilization of process models may be the most convenient way to improve the process performance (Yeo et al. [1]). Various methods of modeling the paper drying process have been proposed. Depoy [2] presented a simple analog model describing heat capacity, heat conductivity and heat transfer coefficients. The model employs mass and energy balances for the paper web structure. Another way of representing moisture content and bone dry mass is to employ steam pressure, velocity of drying cylinders and cylinder temperatures (Berrada et al. [3]). Nilsson [4] adopted heat and mass transfer mechanisms in cylinder groups to give a paper drying model. Gardner [5] provided basic principles of modeling of paper drying and showed practical application of those principles in drying equipments. Management of steam pressure during a paper grade change operation is very important and Magnus [6] presented dynamic modeling simulations of steam supplying systems for multiple drying cylinders during a grade change operation. Sivill [7] tried to reduce operational cost based on the thermodynamic modeling of heat recovery rate from drying equipments. Lu et al. [8] presented mathematical and experimental description on the moisture content of the paper web by using heat and mass transport phenomena during phase changes within porous media. Yeo et al. [9] performed numerical simulations using the heat transfer coefficients represented in terms of moisture content, basis weight and reel speed. A description of the overall paper drying process as well as relevant facilities can be found elsewhere (Karlsson [10]).

In this work a dynamic model for paper drying cylinders is developed to evaluate drying performance as well as evaporation efficiency of the paper drying section. Results of numerical simulations are compared with operation data.

1. Dynamic Models for Drying Cylinders

Drying of paper web can be considered as a combination of heat and mass transfer phenomena. The energy of steam is transferred to the paper web via drying cylinder wall followed by evaporation of water from the surface of the web. The model includes a mass balance for the cylinder and a description of the flow through the valve. The following assumptions were made:

- The steam inside the drying cylinder is saturated.
- Pressure drops caused by pipes are very small.
- Changes in condensate film thickness are small.
- The steam supply pressure is constant.
- Valve changes are instantaneous.
- Temperature and pressure gradients within the cylinder cavity are negligible.

The drying cylinder is heated by the steam supplied from steam distribution facilities. Obviously, the inner temperature of the cylinder is higher than that of the paper web. Fig. 2 shows the temperature profile and energy flows for the cylinder. In Fig. 2, T_s represents steam temperature, T_m denotes the average cylinder temperature and is the web temperature. The amount of steam and water in the drying cylinder is given by:

$$\frac{d}{dt}(\rho_s V_s) = q_s - q_c - q_{bt} \tag{1}$$

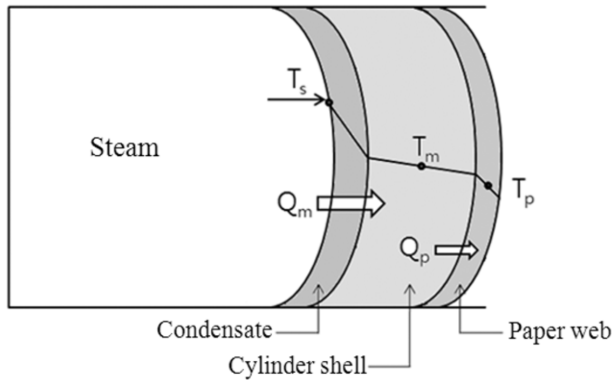

Fig. 2. The temperature profile and the energy flows for a drying cylinder.

$$\frac{d}{dt}(\rho_w V_w) = q_c - q_w \tag{2}$$

where q_s represents steam rate supplied to the cylinder, and q_c and q_{bt} denote rates of condensing and blow-through steam, respectively. q_w is the flow rates of condensate removed by siphon and V_s and V_w are volumes of steam and condensate, respectively. The volume occupied by steam and condensate is given by:

$$V = V_s + V_w \tag{3}$$

The steam rate supplied to the drying cylinder is a manipulated variable adjusted by the steam valve and is represented by:

$$q_s = c_v f_v(X)\sqrt{(p_{sh} - p)\rho_s} \tag{4}$$

where c_v is the valve coefficient and the valve is assumed to be equal percentage valve in which $f_v(X) = R_v^{X-1}$. Energy balances for steam, water content and drying cylinder can be written as:

$$\frac{d}{dt}(\rho_s u_s V_s) = q_s h_s - q_c h_s - q_{bt} h_s \tag{5}$$

$$\frac{d}{dt}(\rho_w u_w V_w) = q_c h_s - q_w h_w - Q_m \tag{6}$$

$$\frac{d}{dt}(mC_{p,m} T_m) = Q_m - Q_p \tag{7}$$

where u_s and u_w represent internal energy of steam and water respectively, and m and $C_{p,m}$ denote mass and heat capacity of drying cylinder, respectively. The energy flow to the cylinder shell can be represented as:

$$Q_m = \alpha_{sc} A_{cyl}(T_s - T_m) \tag{8}$$

where A_{cyl} is the inner area of the cylinder and α_{sc} is the heat transfer coefficient between condensate and cylinder wall. The energy flow to the paper web can be written as:

$$Q_p = \alpha_{cp} A_{cyl} \eta (T_m - T_p) \tag{9}$$

where η is the fraction of cylinder surface covered by the paper web and α_{cp} is the heat transfer coefficient between cylinder surface and paper web.

Based on the assumptions described before, enthalpy, density and temperature of the steam within the drying cylinder can be represented as a function of pressure (Schmidt [11]):

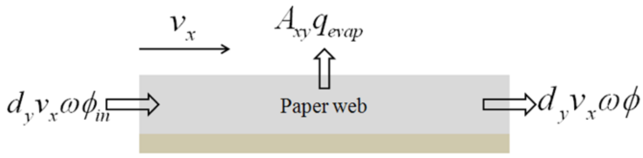

Fig. 3. The moisture balance in the paper web.

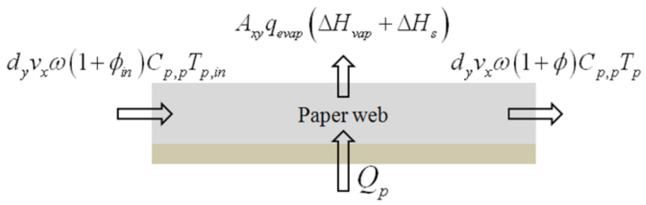

Fig. 4. The energy balance in the paper web.

$$
\begin{aligned}
&T_s=0.1723(\ln p)^3-3.388(\ln p)^2+37.7\ln p+124.5\\
&h_s=[-0.07402(\ln p)^4+2.887(\ln p)^3-39.58(\ln p)^2+260\ln p+1824]\cdot 10^3\\
&h_w=[0.8842(\ln p)^3-18.77(\ln p)^2+200\ln p-748.5]\cdot 10^3\\
&\rho_s=[0.005048p+64.26]\cdot 10^{-3}\\
&\rho_w=-0.3136(\ln p)^3+6.792(\ln p)^2-52.43\ln p+1141
\end{aligned}
\tag{10}
$$

Fig. 3 and Fig. 4 show schematics of mass and energy flow for moisture in the paper web. The mass balance is given by:

$$\frac{d(\phi\omega A_{xy})}{dt}=d_y v_x \omega \phi_{in}-A_{xy}q_{evap}-d_y v_x \omega \tag{11}$$

where v_x is the velocity of the paper web and d_y is the width of the paper web. The evaporation rate can be represented as (Persson [12]):

$$q_{evap}=\frac{p_{tot}KM_w}{gT_p}\ln\left(\frac{p_{tot}-p_{va}}{p_{tot}-p_{vp}}\right) \tag{12}$$

where K is the mass transfer coefficient and M_w is the molecular weight of water. The partial pressure of steam in the air can be represented in terms of the moisture content θ and standard pressure p_{tot}:

$$p_{va}=\frac{\theta}{\theta+0.62}p_{tot} \tag{13}$$

The partial pressure of steam at the web surface is given by:

$$p_{vp}=\varphi p_{v0} \tag{14}$$

The partial pressure of free water p_{v0} can be given by Antoine's equation as $p_{v0}=10^{(10.127-(1690/(T_p-43.15)))}$. The correcting factor, or "sorption isotherm" φ for web drying can be found from experimental results (Heikkilä [13]). Usually φ takes a value between 0 and 1.

$$\varphi=1-\exp(-47.58\phi^{1.877}-0.10085(T_p-273)\phi^{1.0585}) \tag{15}$$

The heat loss due to evaporation at the paper web can be ignored because only conduction and radiation are significant. Moreover, changes in moisture volume due to the pressure can be ignored and we have energy balance given by (see Fig. 3):

$$
\begin{aligned}
\frac{d(\omega(\phi+1)A_{xy}C_{p,p}T_p)}{dt}&=d_y y_x \omega(1+\phi_{in})C_{p,p}T_{p,in}+Q_p\\
&-A_{xy}q_{evap}(\Delta H_{vap}+\Delta H_s)-d_y v_x \omega(1+\phi)C_{p,p}T_p
\end{aligned}
\tag{16}
$$

where ΔH_{vap} is the latent heat of evaporation and $C_{p,p}$, the heat capacity of paper web is given by $C_{p,p}=((C_{p,fiber}+\phi C_{p,w})/(1+\phi))$. The excess energy ΔH_s can be represented by Clausius-Clapeyron relation derived from the sorption isotherm:

$$\Delta H_s=-\frac{g}{M_w}\left[\frac{d(\ln\varphi)}{d(1/T_p)}\right] \tag{17}$$

Substitution of Eq. (15) into Eq. (17) gives

$$\Delta H_s=0.10085\phi^{1.0585}T_p^2 g\frac{\varphi-1}{M_w\varphi} \tag{18}$$

The steam rate manipulated by the steam valve alters the steam pressure within the drying cylinder followed by changes of tem-

Table 1. Basic data for a typical drying cylinder

Description	Numerical value
Cylinder volume [m^3]	12.6
Cylinder mass [kg]	7610
Cylinder area [m^2]	45.5
Specific heat capacity of paper [J/(kg·K)]	1256
Latent heat of vaporization [kJ/kg]	2260
Speed of machine [m/min]	1300
Basis weight [g/m^2]	77
Initial dryness [%]	55
Steam header pressure [kPa]	510

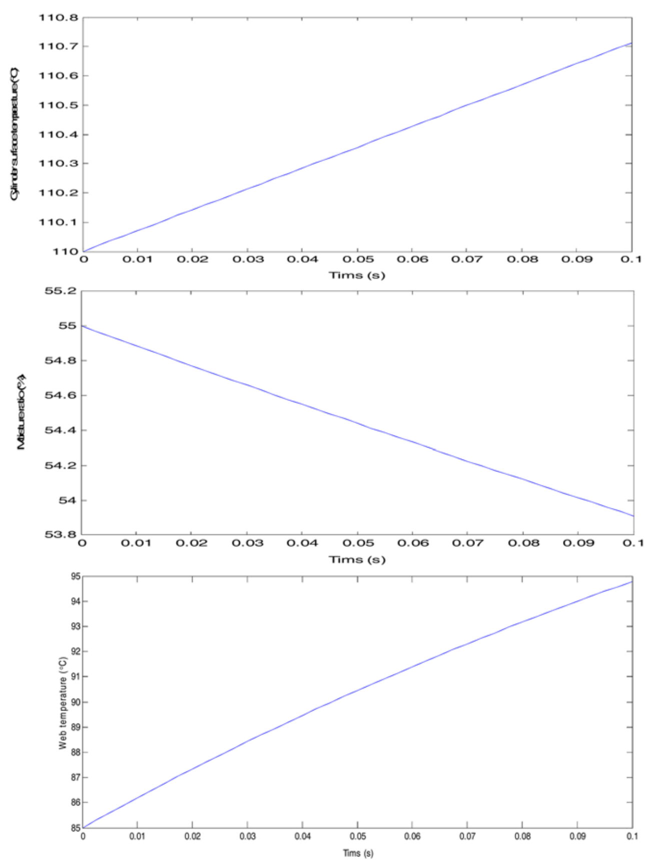

Fig. 5. Results of simulations for single drying cylinder (basis weight: ω=77 g/m^2).

perature and moisture content in the paper web. Based on the present model, variation of temperatures of the cylinder surface and the paper web and behavior of moisture content of the paper web are investigated for the paper with basis weight of ω=77 g/m^2 and initial moisture content of 55%. Table 1 shows data used in numerical simulations and Fig. 5 displays results of computations.

A typical drying section consists of drying cylinders and felt rolls arranged in two rows. The paper web moves between upper cylinders and lower cylinders alternately. A dryer fabric or a felt is used to press the paper web toward the drying cylinder being heated by steam. In general, the drying section contains 30-70 drying cylinders. The model for multi-cylinder drying section can easily be obtained by direct extension of the single-cylinder model with incorporation of the configuration types (single-tier type, single-felted type and double-felted type).

As a test case to demonstrate the model, we now consider an artificially constructed drying section which is equipped with 39 drying cylinders of which the first 26 cylinders are assembled in single-tier type and the remaining 13 cylinders are assembled in doubled-felted type. The cylinders are divided into four groups, depending on the steam pressure being supplied. Operating conditions and relative data for numerical simulations are given in Tables 2 and 3. The initial moisture content of the paper web was assumed to be 45%.

A typical operation case was examined for the purpose of comparison and verification of the present model. The key operating variables being measured are temperature and moisture content. Measured values of these variables are compared with those computed from the present model. The operation case is based on the operation at the plant in Shinmoorim Paper Company, Jinju, Korea. Machine speed is 1,420 m/min and the basis weight is 62 g/m^2. All the drying cylinders are arranged in single-tier type. Tables 4 and 5 show the operating conditions and configuration of the operating case.

Table 2. Simulation data for the dryer section

Description	Numerical value
Reel speed [m/min]	1044
Basis weight [g/m^2]	41
Steam to the 1st group [kPa]	69
Steam to the 2nd group [kPa]	152
Steam to the 3rd group [kPa]	206
Steam to the 4th group [kPa]	206

Table 3. Configuration of the dryer section

Section	Group number	Cylinders	Remarks
Main dryer	1	1-7	Single-tier configuration
	2	8-19	
	3	20-26	
	4	27-39	Double-felted configuration

Table 4. Basic data for the operation case

Description	Numerical value
Reel speed [m/min]	1420
Basis weight [g/m^2]	62
Steam to the cylinder No. 1-3 [kPa]	14
Steam to the cylinder No. 4 [kPa]	36
Steam to the cylinder No. 5-9 [kPa]	132
Steam to the cylinder No. 10-16 [kPa]	162
Steam to the cylinder No. 17-31 [kPa]	226
Steam to the cylinder No. 32-33 [kPa]	212
Steam to the cylinder No. 34-4 [kPa]	377

Table 5. Configuration of the dryer section for the operation case

Section	Group number	Cylinders	Remarks
Main dryer	1	1-4	Single-tier configuration
	2	5-15	
	3	16-31	
	4	32-33	
	5	34-40	

2. Generation of Entropy

The conservation equation for the moisture content per unit area can be written as:

$$\frac{d\phi}{dt}=\frac{1}{\omega}q_{evap} \tag{19}$$

The balance equation for the internal energy is given by

$$\frac{dh_p}{dt}=\frac{1}{\omega}(J_{cp}+J_{pa}-q_{evap}h^{air}_{H_2O}(T_a)) \tag{20}$$

where $h^{air}_{H_2O}$ denotes the specific enthalpy of vapor represented as a function of the ambient temperature T_a. The specific enthalpy h_p of the paper web is assumed to be a combination of the enthalpy of the dry web $h_{p,dry}$ and the enthalpy of the vapor contained in the paper web $h^{paper}_{H_2O}$. Then h_p can be represented as

$$h_p=h_{p,dry}(T_p)+\phi h^{paper}_{H_2O}(T_p,\phi) \tag{21}$$

The rate of change of h_p with time is given by

$$\begin{aligned}\frac{dh_p}{dt}&=\frac{\partial h_p}{\partial T_p}\frac{dT_p}{dt}+\frac{\partial h_p}{\partial\phi}\frac{d\phi}{dt}=C_{p,p}\frac{dT_p}{dt}+\frac{\partial(\phi h^{paper}_{H_2O}(T_p,\phi))}{\partial\phi}\frac{d\phi}{dt}\\&=C_{p,p}\frac{dT_p}{dt}-\frac{q_{evap}}{\omega}h^{air}_{H_2O}(T_a)+\frac{q_{evap}}{\omega}\frac{\partial(\phi\Delta H)}{\partial\phi}\end{aligned} \tag{22}$$

Equating Eq. (22) with Eq. (20) and substituting Eq. (19) gives

$$\frac{dT_p}{dt}=\frac{1}{\omega C_{p,p}}\left(J_{cp}+J_{pa}-q_{evap}\frac{\partial(\phi\Delta H)}{\partial\phi}\right) \tag{23}$$

The rate of the entropy production σ can be written as

$$\sigma=\omega\frac{ds_p}{dt}-\frac{J_{cp}}{T_m}-\frac{J_{pa}}{T_a}-q_{evap}s^{air}_{H_2O}(T_a) \tag{24}$$

The specific entropy s_p of the paper web can be represented in terms of the specific entropy $s_{p,dry}$ and the specific entropy $s^{paper}_{H_2O}$ of vapor contained in the web.

$$s_p=s_{p,dry}(T_p)+\phi s^{paper}_{H_2O}(T_p,\phi) \tag{25}$$

Thus the rate of change of s_p with time is given by

$$\frac{ds_p}{dt}=\frac{\partial s_p}{\partial T_p}\frac{dT_p}{dt}+\frac{\partial s_p}{\partial \phi}\frac{d\phi}{dt}=\frac{C_{p,p}}{T_p}\frac{dT_p}{dt}+\frac{\partial(\phi s^{paper}_{H_2O}(T_p,\phi))}{\partial \phi}\frac{d\phi}{dt}$$
$$=\frac{C_{p,p}}{T_p}\frac{dT_p}{dt}-\frac{q_{evap}}{\omega}s^{air}_{H_2O}(T_a)+\frac{q_{evap}}{\omega}\frac{\partial(\phi\Delta S)}{\partial \phi} \qquad (26)$$

Substitution of Eqs. (19), (23) and (25) into Eq. (26) gives after some rearrangement

$$\sigma=J_{cp}\left(\frac{1}{T_p}-\frac{1}{T_m}\right)+J_{pa}\left(\frac{1}{T_p}-\frac{1}{T_a}\right)+q_{evap}\left(-\frac{1}{T_p}\frac{\partial(\phi\Delta H)}{\partial\phi}+\frac{\partial(\phi\Delta S)}{\partial\phi}\right) \qquad (27)$$

The heat flux J_{cp} from the cylinder to the paper web and the heat fluxes J_{pa} from the paper web to the environment can be represented in terms of respective heat transfer coefficients α_{cp} and α_{pa}.

$$J_{cp}=\alpha_{cp}(T_m-T_p) \qquad (28)$$

$$J_{pa}=\alpha_{pa}(T_a-T_p) \qquad (29)$$

The amount of entropy production, σ, must be positive according to the 2nd law of thermodynamics. The first two terms on the right-hand side of Eq. (27) give the contributions to the entropy production from the heat transfer, while the last term gives the contribution from the mass transfer. From this observation we can now identify thermodynamic driving forces and fluxes acting in the multi-cylinder paper drying process. The driving forces for heat transport are the first two terms on the right-hand side of Eq. (27), and the driving force for mass transport is the last expression on the right-hand side of Eq. (27). Integration of Eq. (27) over the total length of the paper web, from the wet to the dry-end of the drying machine, gives the total entropy production in the drying process.

RESULTS AND DISCUSSION

Models consist of ordinary differential equations coupled with algebraic relations. The ODE toolbox of MATLAB (v. R2009a) was used as the solver for these modeling equations. Variations in the temperatures of the cylinder surface and the paper web as well as in the moisture content of the paper web for single drying cylinder are shown in Fig. 5. If the steam pressure is maintained constant, temperatures exhibit steady increase followed by steady decrease in the moisture content of the paper web. Behavior of each drying cylinder is dependent upon the configuration type of drying cylinders and the paper web.

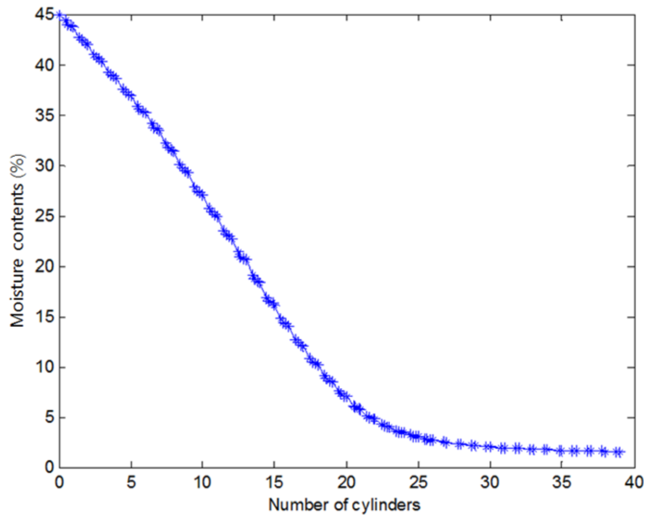

Fig. 7. Results of moisture content calculations for the example case (basis weight: ω=41 g/m^2).

Figs. 6 and 7 show results of simulations for the example case set up to test the model. Fig. 6 shows the behavior of temperatures of cylinder surfaces and the paper web. Temperatures of the paper web and of cylinder surfaces increase steadily as the web transfers through drying cylinders. As can be seen, the web temperature exhibits sharp increase as the web moves from the 2nd group to the 3rd group. This increase is caused by the difference of the steam pressure supplied to each group. The double-felted cylinder group exhibits smaller temperature differences between the cylinder contacting region and free-run region compared to temperature variations within the single-tier group. Fig. 7 shows variations of moisture content within the paper web. We can see that the evaporation rate increases in the region where the web temperature shows a sharp increase.

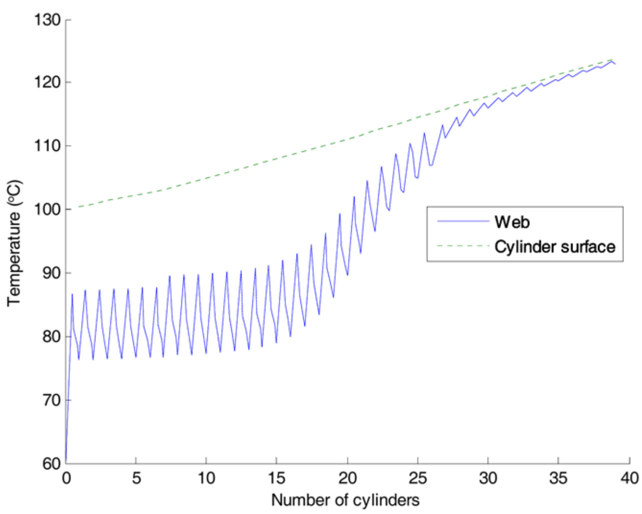

Fig. 6. Results of temperature calculations for the example case (basis weight: ω=41 g/m^2).

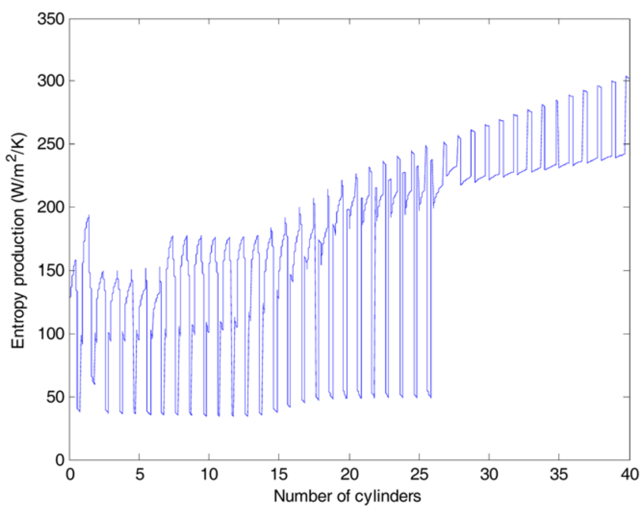

Fig. 8. Results of entropy calculations for the example case (basis weight: ω=41 g/m^2).

Fig. 8 shows the results of entropy computations. The entropy production shows similar behavior with that of the web temperature. The entropy production varies as the paper web moves through cylinder surface, free-run region and vacuum rolls due to the difference in energy the web receives. In fact, the profile of the entropy production exhibits a zig-zag pattern, which reaches peak values at the beginning of each drying group. At these positions, the heating conditions are changed. Different cylinder configurations cause variations in entropy production at the 3rd and 4th cylinder group. Integration under the curve shown in Fig. 8 gives the total entropy production in the drying process for the specific paper grade.

Figs. 9-10 show the results of numerical simulations as well as the operation data for the operation case. Operation data are denoted by small circles. As can be seen in Fig. 9, computation results for the web temperatures track operation data pretty well. Fig. 10 shows the entropy production. The value of the entropy production around 25th cylinder decreases, while the web temperature at this region is higher than neighboring cylinders. This is because variations in temperatures around 25th cylinder are lower than those at other regions. The sharp variation of the entropy production around the gate roll compared to that around the main dryer section seems to be caused by the difference in the heat transfer coefficients between these regions. Normally, the heat transfer coefficient around the main dryer section is much larger than that around the gate roll. In fact, rigorous estimation of energy consumption, although not performed in this work, is possible by the measurement of temperatures and heat transfer coefficients.

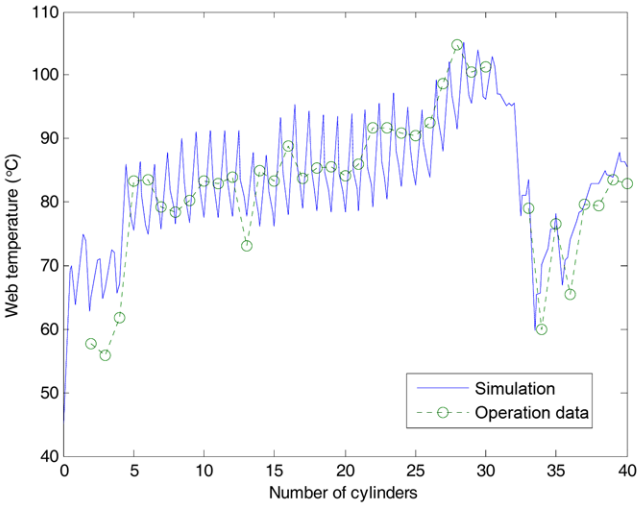

Fig. 9. Comparison between numerical simulations and operating data for the operation case (basis weight: ω=62 g/m^2).

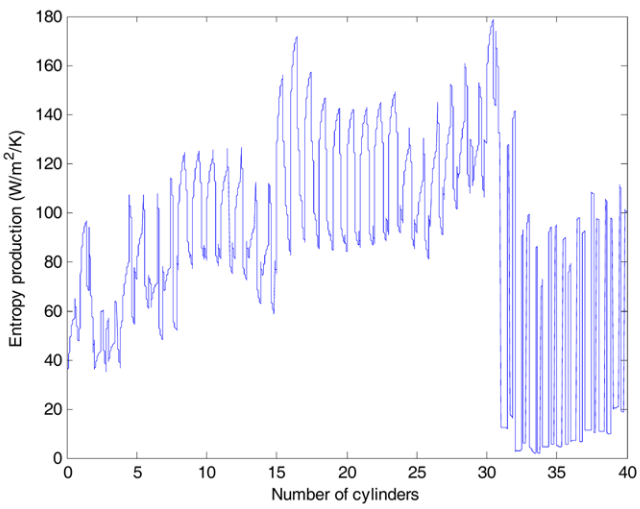

Fig. 10. Entropy production for the operation case (basis weight: ω=62 g/m^2).

CONCLUSIONS

A model for multi-cylinder drying processes can be obtained by direct extension of the single cylinder model, which is based on the mass and heat balances around the cylinder. The balance equations for single drying cylinder consist of sets of differential equations describing heat and mass transfer around the canvas, the web and the drying cylinder. Incorporation of configuration types of drying cylinders completes the model for the multi-cylinder drying section. Variations in cylinder surface temperatures and values of entropy production at each cylinder were examined for the multi-cylinder drying process. For the purpose of comparison, a typical operating case was examined. It was found that the present multi-cylinder model represents the operation data very well.

ACKNOWLEDGEMENT

This work was supported by Korea Research Foundation Grant funded by the Korean Government (KRF-2008-313-D00177).

NOMENCLATURE

A_{cyl} : inner cylinder area [m^2]
A_{xy} : area of paper covering the cylinder [m^2]
C_v : valve conductance [m^2]
$C_{p,fiber}$: specific heat capacity of fiber (=1256) [J/(kg·K)]
$C_{p,m}$: specific heat capacity of cylinder shell [J/(kg·K)]
$C_{p,p}$: specific heat capacity of the paper [J/(kg·K)]
$C_{p,w}$: specific heat capacity of water [J/(kg·K)]
d_y : width of paper sheet [m]
g : gas constant [J/(mole·K)]
$h^{air}_{H_2O}$: specific enthalpy of vapor [J/kg]
h_p : specific enthalpy of the paper web [J/kg]
h_s : enthalpy of steam [J/kg]
h_w : enthalpy of condensate [J/kg]
k_c : thermal conductivity of cylinder [J/m·K]
k_p : thermal conductivity of paper [J/m·K]
J_{cp} : heat fluxes from cylinder to paper [kg/(m^2·s)]
J_{pa} : heat fluxes from paper to air [kg/(m^2·s)]
K : mass transfer coefficient for paper sheet [m/s]
m : mass of cylinder shell [kg]
M_w : molecular weight of water [kg/mole]
p : steam pressure inside cylinder [kPa]
p_{sh} : steam pressure in header [kPa]
p_{tot} : standard pressure (=101.325) [kPa]
p_{v0} : partial vapor pressure for free water [kPa]

p_{va} : partial pressure for water vapor in the air [kPa]
p_{vp} : partial pressure for water vapor at paper surface [kPa]
q_{bt} : blow through steam [kg/s]
q_c : condensation rate [kg/s]
q_{evap} : evaporation rate [kg/(m^2·s)]
q_s : inflow of steam to cylinder [kg/s]
q_w : outflow of condensate [kg/s]
Q_m : energy flow to cylinder shell [W]
Q_p : energy flow to paper [W]
R_v : valve rangeability [-]
s_p : specific entropy of paper [J/kg/s]
$s_{H_2O}^{paper}$: specific entropy of vapor contained in the web [J/kg/s]
T_a : temperature of air [K]
T_m : temperature of cylinder shell [K]
T_p : temperature of paper [K]
T_s : temperature of steam [K]
u_s : internal energy of steam [J/kg]
u_w : internal energy of condensate [J/kg]
v_x : speed of paper sheet [m/s]
V : volume inside cylinder [m^3]
V_s : volume of steam [m^3]
V_w : volume of condensate [m^3]
X : valve opening [-]

Greek Letters

α_{cp} : heat transfer coefficient cylinder-paper [W/(m^2·K)]
α_{pa} : heat transfer coefficient paper-air [W/(m^2·K)]
α_{sc} : heat transfer coefficient steam-cylinder [W/(m^2·K)]
ΔH : enthalpy change [J/kg]
ΔH_s : heat of sorption [J/kg]
ΔH_{vap} : latent heat of vaporization [J/kg]
ΔS : entropy change [J/kg/s]
ϕ : moisture ratio [kg/kg]
φ : sorption isotherm [-]
η : fraction of dryer surface covered by paper [-]
θ : water content in air [kg/kg]
ρ_s : density of steam [kg/m^3]
ρ_w : density of condensate [kg/m^3]
σ : entropy production [W/m^2·K)]]
ω : dry basis weight of paper [kg/m^2]

REFERENCES

1. Y. K. Yeo, H. D. Roh, I. W. Kim and Y. Chung, *Korean J. Chem. Eng.*, **20**, 200 (2003).
2. J. A. Depoy, *Pulp & Paper Magazine of Canada*, **73**, 67 (1972).
3. M. Berrada, S. Tarasiewicz, M. E. Elkadiri and P. H. Radziszewsk, *IEEE Trans. Ind. Electron.*, **44**, 579 (1997).
4. L. Nilsson, *Chem. Eng. Process.*, **43**, 1555 (2004).
5. M. Grander, *Computer simulation of the dryer section*, Albany international, Paper Technology (2000).
6. K. Magnus, *Nordic Pulp and Paper Research Journal*, 17 (2002).
7. L. Sivill and P. Ahtila, *Thermal Engineering*, **29**, 3663 (2009).
8. T. Lu and S. Q. Shen, *Thermal Engineering*, **27**, 1248 (2007).
9. Y. K. Yeo, K. S. Hwang, S. C. Yi and H. Kang, *Korean J. Chem. Eng*., **21**(4), 761 (2004).
10. M. Karlsson, Papermaking Science and Technology Book 9, Fapet Oy., 55 (2002).
11. E. Schmidt, *Properties of water and steam in SI-units*, Springer Verlag, Berlin, Germany (1969).
12. H. Persson, *Dynamic modeling and simulation of multi-cylinder paper dryers*, Licentiate Thesis, Department of Chemical Engineering, Lund Institute of Technology (1998).
13. P. Heikkilä, *A study on the drying process of pigment coated paper webs*, PhD Thesis, Department of Chemical Engineering, Åbo Akademi, Åbo, Finland (1993).